

# Shallow subsurface characterization using high frequency ambient noise at Terziet, Limburg

---

Soumen Koley, Xander Campman,  
Shahar Shani Kadmiel,  
Bjorn Vink, Frank Linde  
GSSI, Nikhef

[soumen.koley@gssi.it](mailto:soumen.koley@gssi.it)

[skoley@nikhef.nl](mailto:skoley@nikhef.nl)

# An array of 183 vertical component 5 Hz geophones deployed between Nov. 12 – Dec 06, 2020

- Array covers an approximate area of 7x7 sq. km
- Approximate station separation of about 300-400 m

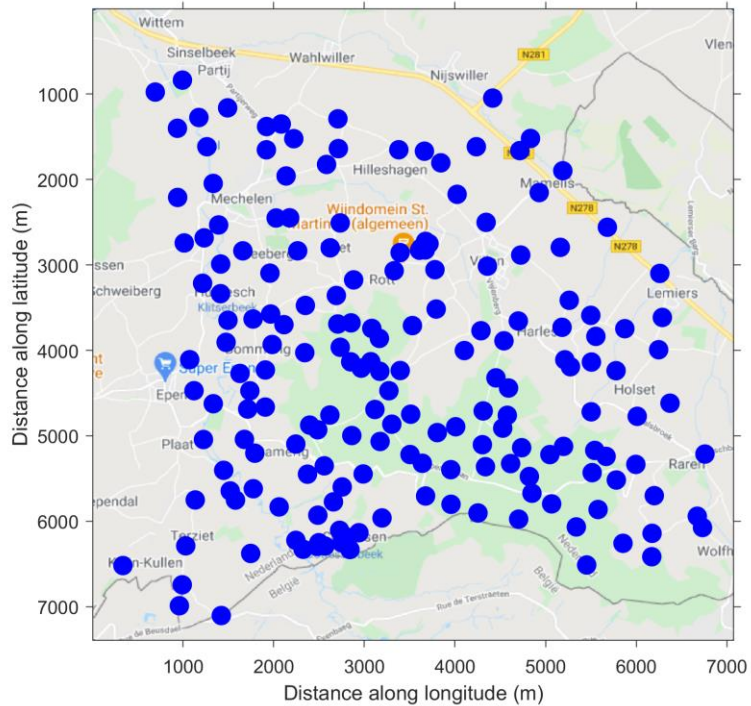
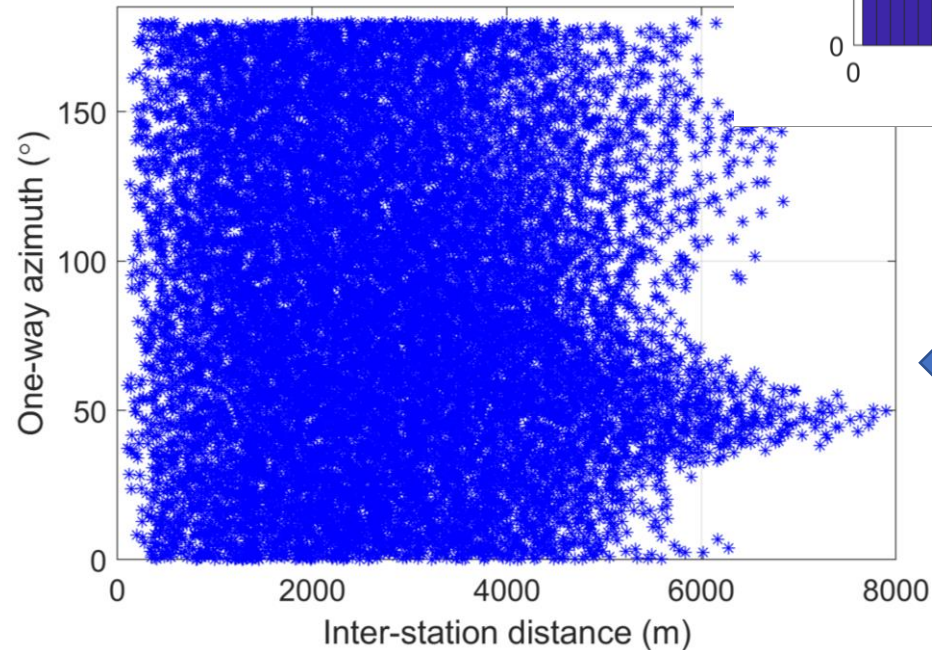
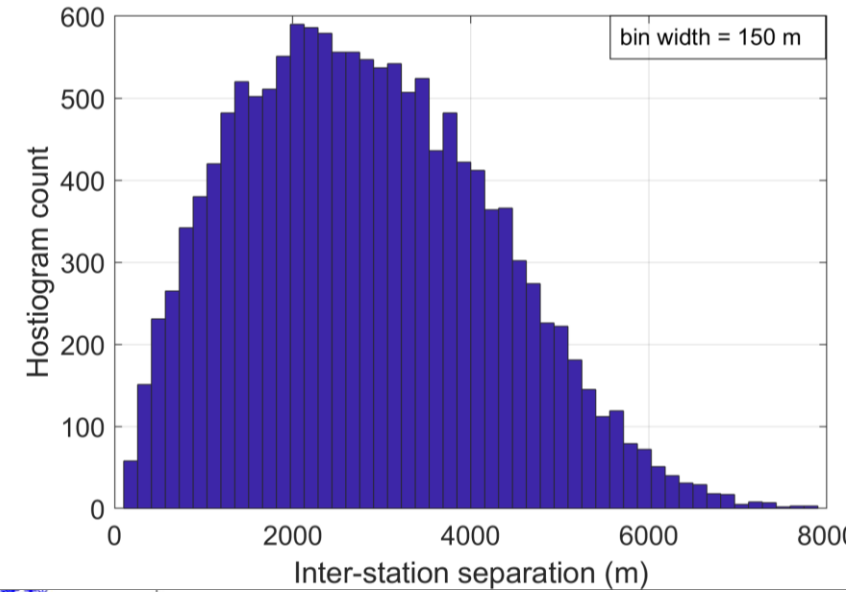


**Figure: Sensor locations overlaid on a map of the region**

- Adequate station-pairs with interstation distances in the range 1 – 4.5 km for array analysis and interferometry at low frequencies



- Good azimuthal coverage for all inter-station distances up to 6 km which is important for tomography





# Noise PSD characteristics(>1 Hz)

- PSD parameters:
  - Window length – 600 s (50 Hz)
  - Overlap length – 300 s
  - Windowing function
    - Tukey,  $\alpha = 0.1$

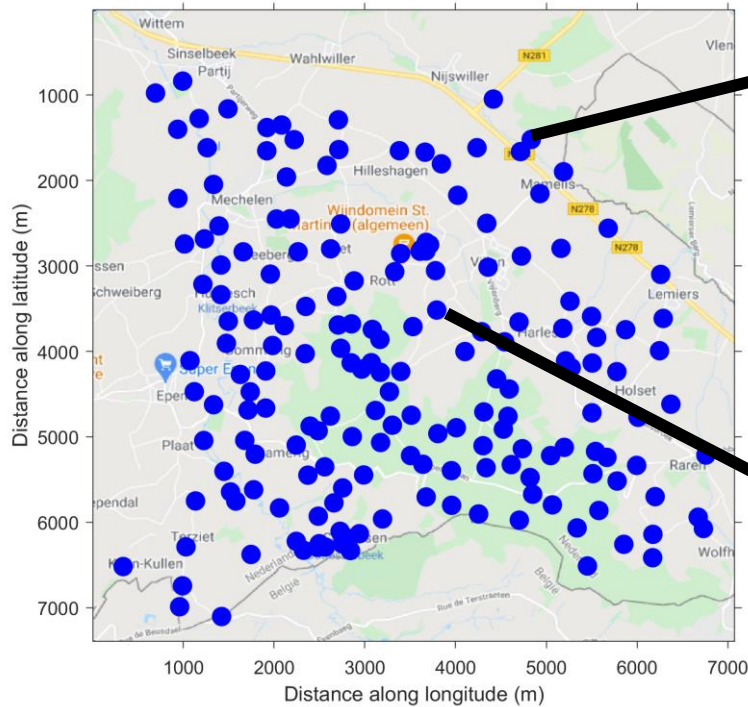
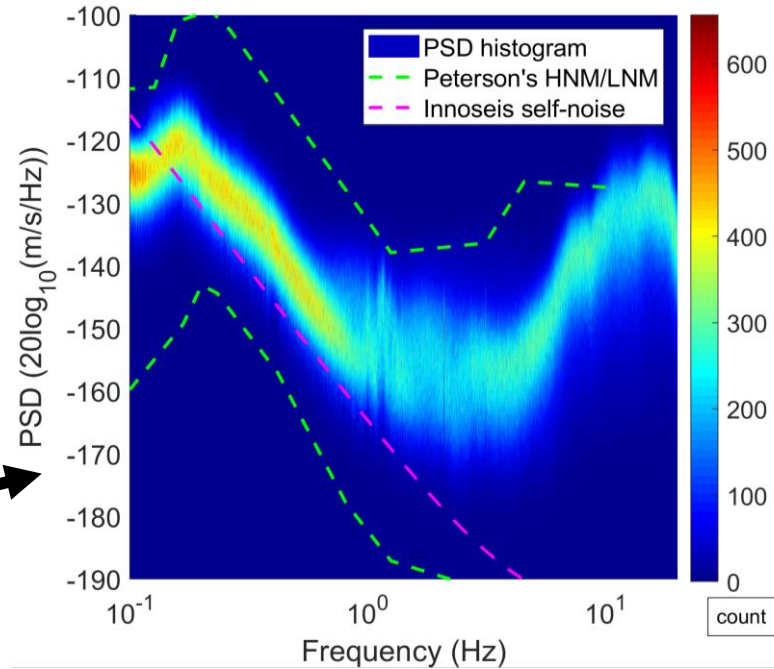
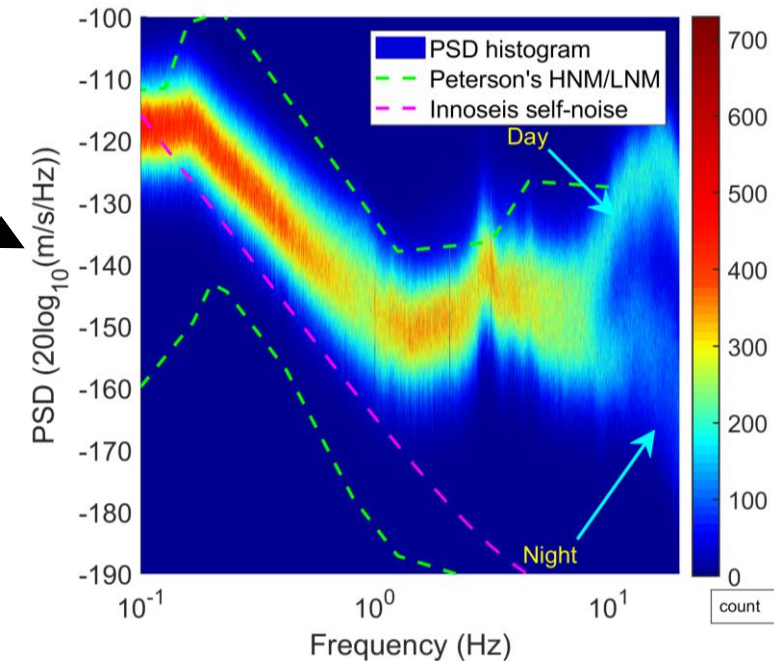


Figure: Sensor locations overlaid on a map of the region



- Station Z2KWA stationed in the vicinity of highway N-278 measures a persistent high-level of ambient noise
- No significant day-night variation is observed
- Noise below 1 Hz “might” be sensor self-noise limited



- Station ZCM4A stationed in the vicinity of a local road and exhibits a typical day and night variation
- A variation of about 40 dB in power is observed

Related Literature: [McNamara & Buland 2004](#), [Groos & Ritter, 2009](#)

## Noise PSD characteristics(>1 Hz)

- Figure below showing two stations situated away from anthropogenic noise sources like roads, industrial noise etc

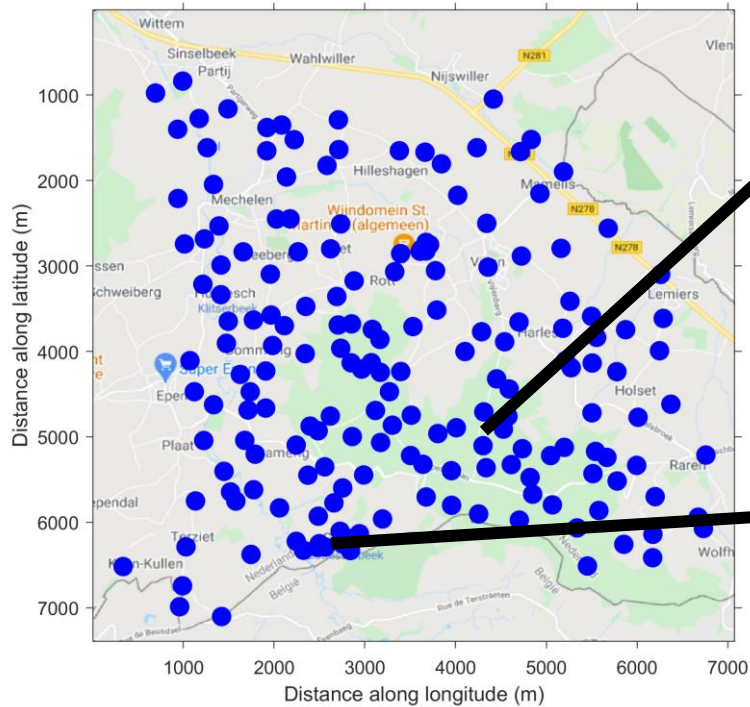
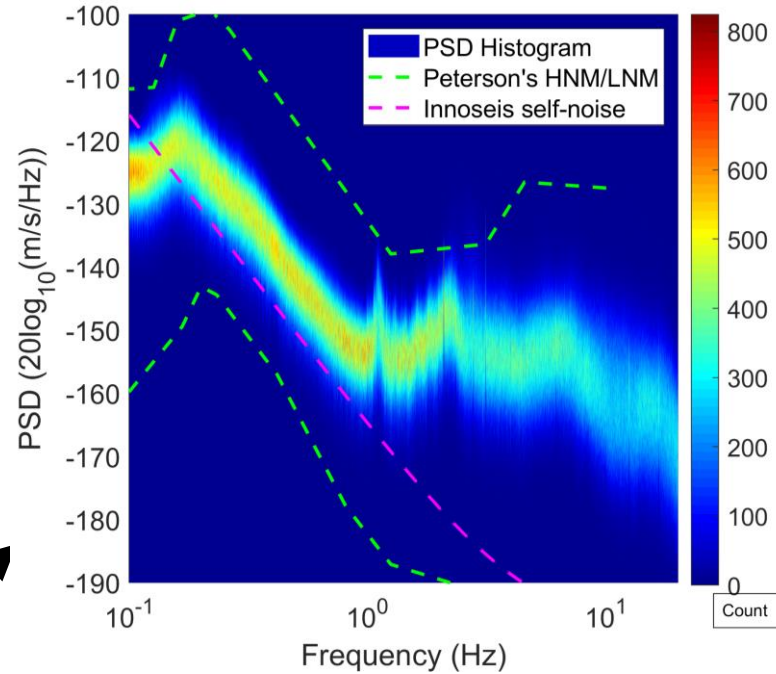
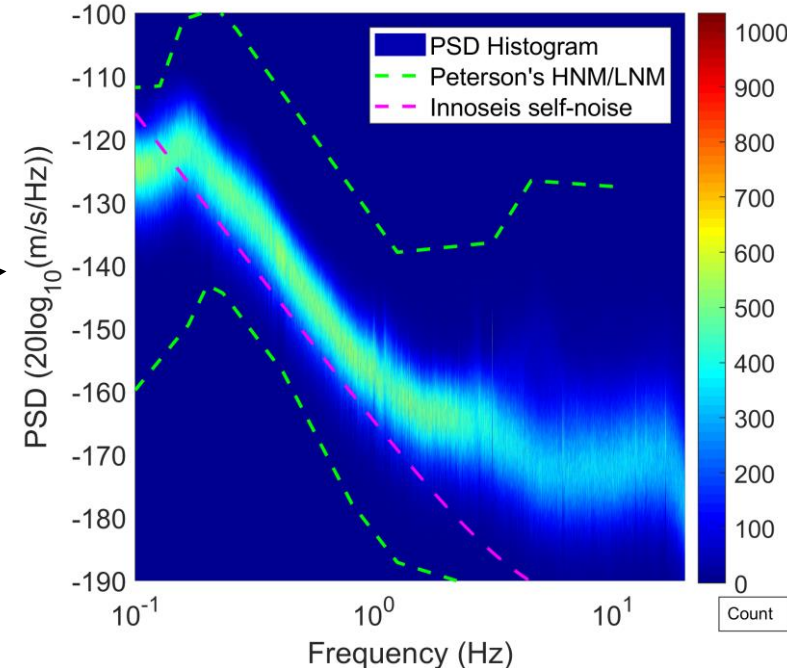


Figure: Sensor locations overlaid on a map of the region



- Station ZQO1A stationed in Vijlenerbos shows low-level of anthropogenic noise
- No dominant day-night variation
- Broad spectral peaks at 1.2 Hz, 2.3 Hz, and 3.1 Hz originating from windmills are visible
- The drop in noise below 0.2 Hz is due to pre-filtering applied to the data during instrument-response removal



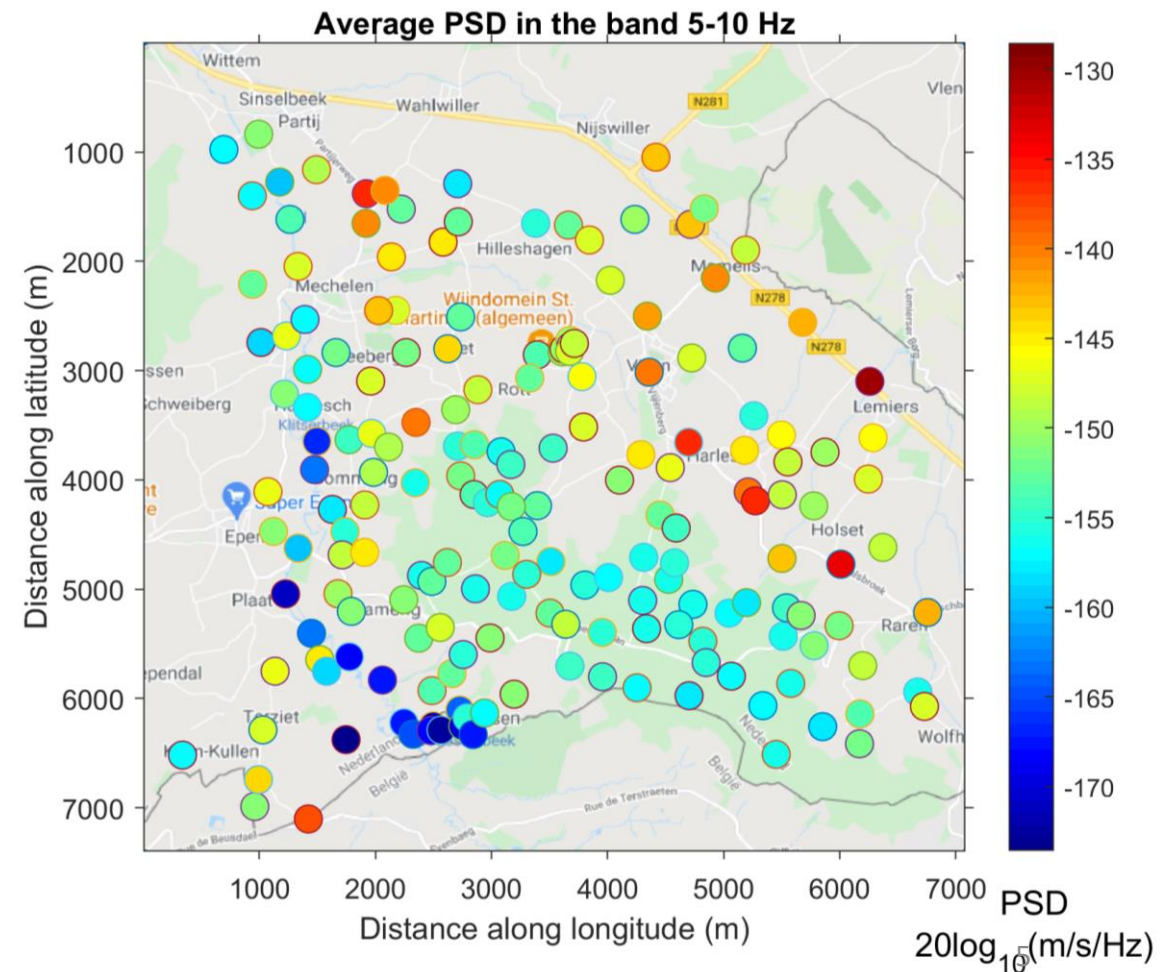
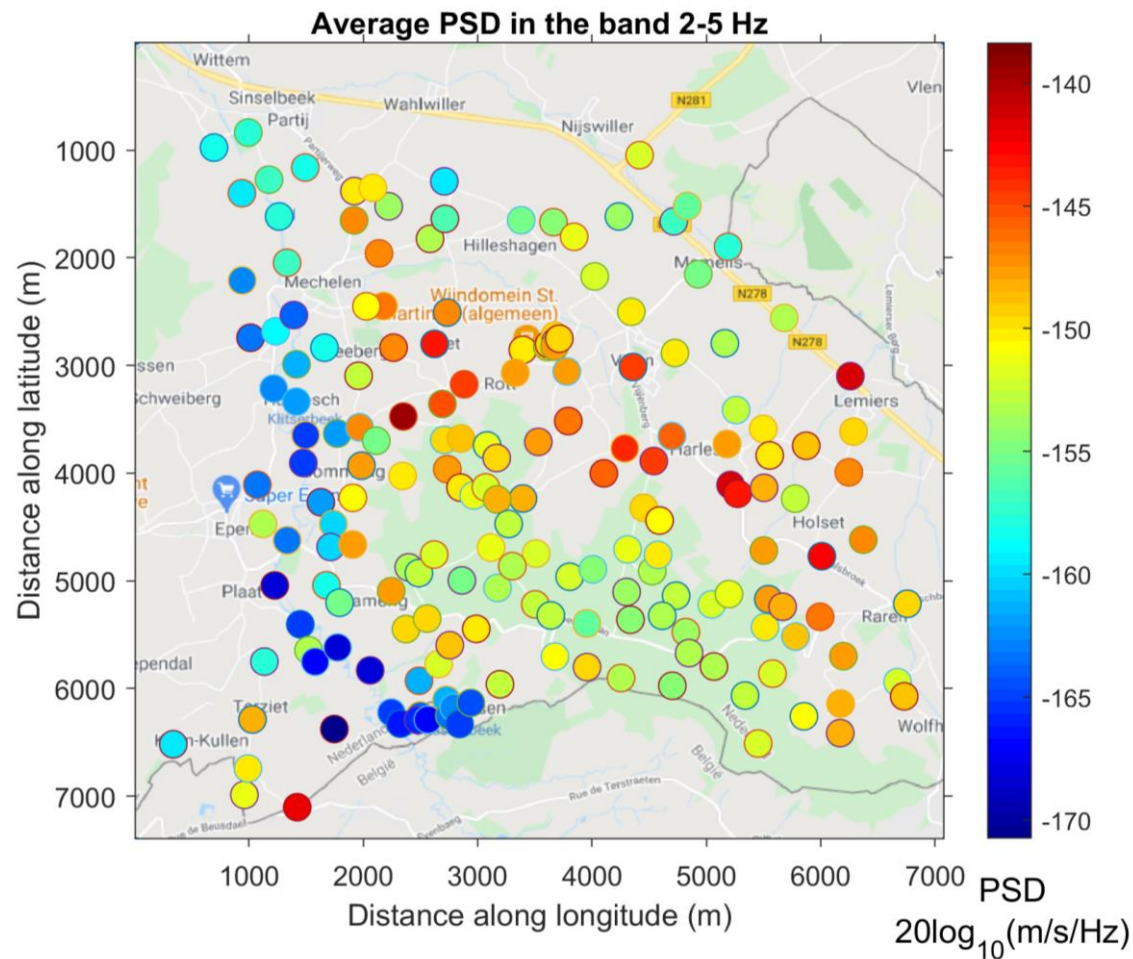
- Station YCQGA stationed at Cottessen measures a low-level of ambient noise and about 50 dB lower in power as compared to noisy stations
- The station is located at a site with only a few meters of soft soil, resulting in little amplification of surface-generated anthropogenic noise

Related Literature: [Seo, 1997](#)



# Spatial variation of average PSD in the frequency band 2-5 Hz and 5-10 Hz

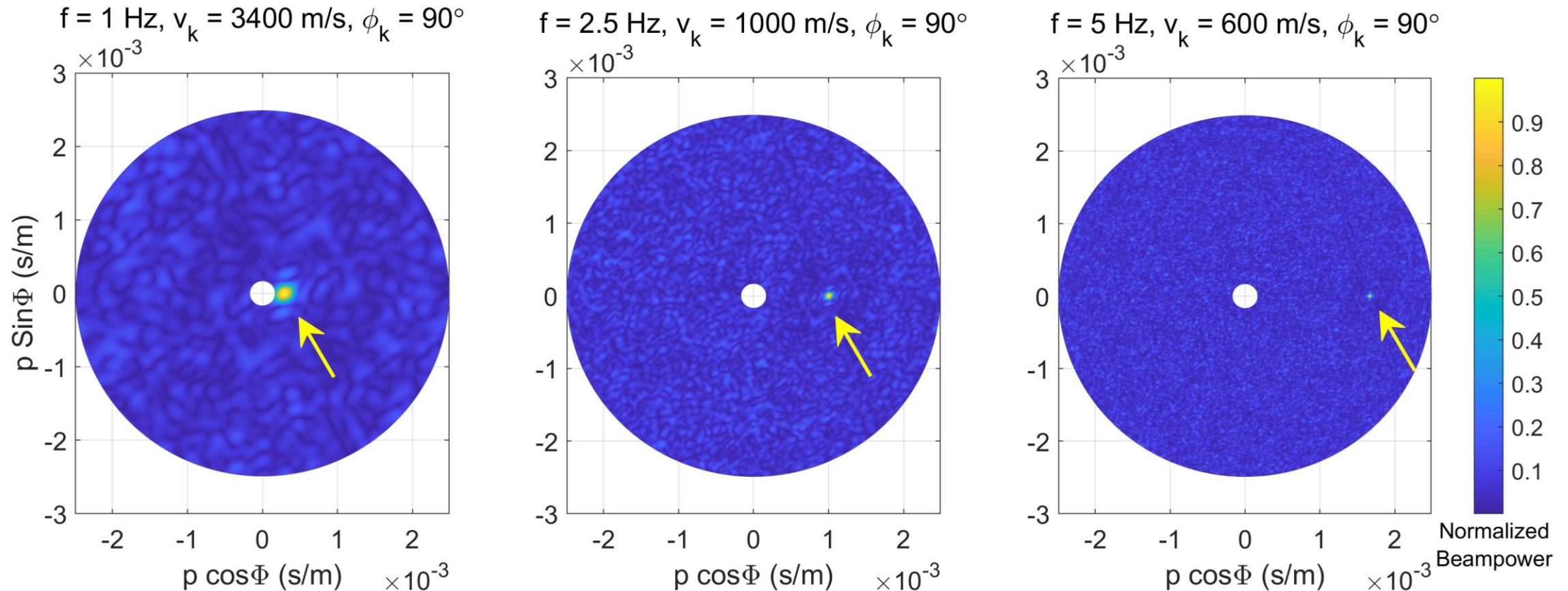
- Spatial variation of PSD of about 30 dB observed in the band 2-5 Hz
- This variation increases to about 50 dB for the band 5-10 Hz
- Low-levels of anthropogenic noise observed at hard-rock sites and *valley-like setting* ([Panzera et al 2011](#))



# Array processing

**Theoretical array response** – Given plane wave incidence under conditions that the wave suffers no attenuation during propagation, the array can sample up to 5 Hz and velocities of about 600 m/s

- $AR_{TH}(v_k, \phi_k, f) = A(f) \times a_k^*(f)$ , where  $A(f) = [a_0(f), a_1(f), \dots, a_{N_p N_\phi}(f)]$ , and  $a_k(f) = [e^{2\pi f j \tau_{0,k}}, e^{2\pi f j \tau_{1,k}}, \dots, e^{2\pi f j \tau_{M,k}}]$ , and  $j = \sqrt{-1}$ , " \* " represents complex conjugate
- $\tau_{m,k} = x_m p_k \cos \phi_k + y_m p_k \sin \phi_k$ ,  $(x_m, y_m)$  are the coordinates of the  $m^{\text{th}}$  station

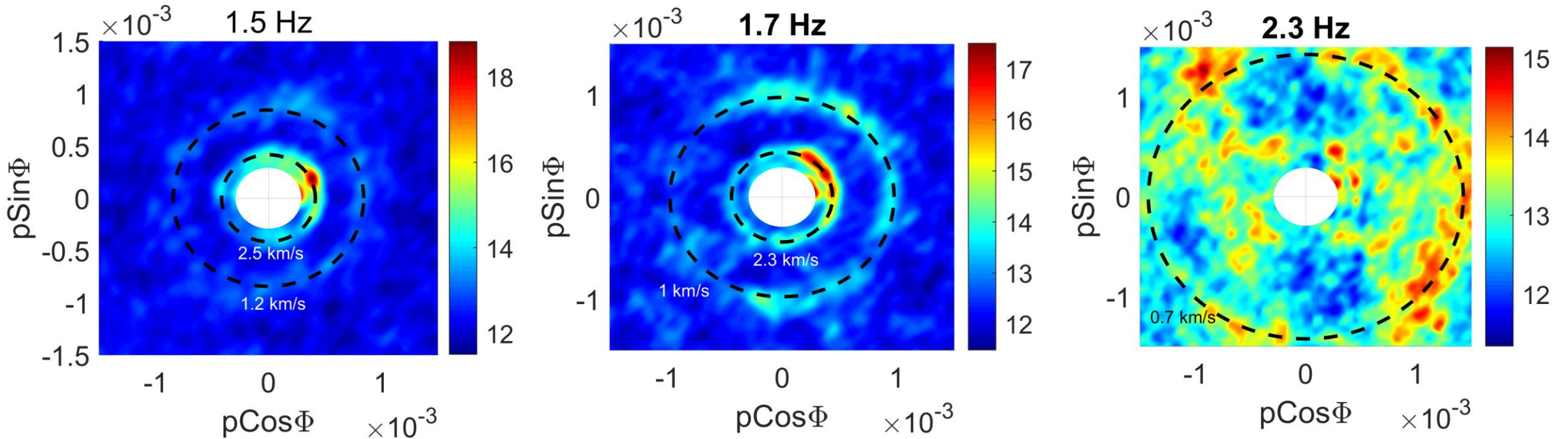


Related Literature: [Lacoss et al, 1969](#)



# Ambient noise beamforming

- Estimating beampower corresponding to different values of speed and azimuth of wave propagation helps infer about the dominant propagation mode of coherent plane waves propagating through an array of seismometers
- $BP(v_k, \phi_k, f) = a_k(f)R_{xx}(f)a_k^*(f)$ , where  $a_k(f) = [e^{2\pi jf\tau_{0,k}}, e^{2\pi jf\tau_{1,k}}, \dots, e^{2\pi jf\tau_{M,k}}]$  and  $\tau_{M,k} = x_M p_k \cos\phi_k + y_M p_k \sin\phi_k$ ,  $p_k = 1/v_k$ ;  $R_{xx}(f)$  is the frequency domain data covariance matrix of size  $M \times M$  where  $M$  represents the number of stations



- A dominant first overtone observed besides a relatively weaker fundamental mode
- Noise illumination – dominantly North-East
- Beampower SNR reduces drastically above 2 Hz – lack of coherent noise

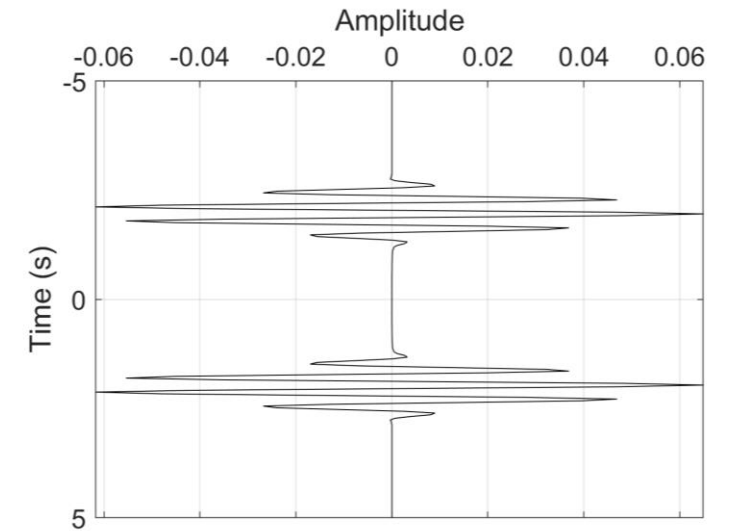
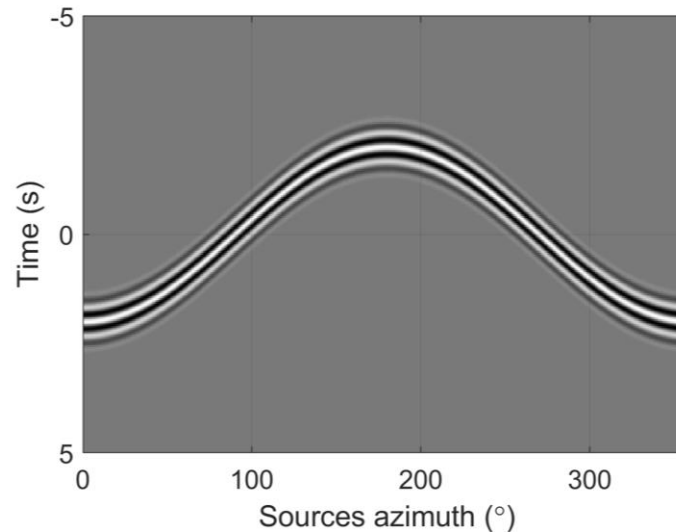
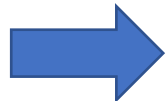
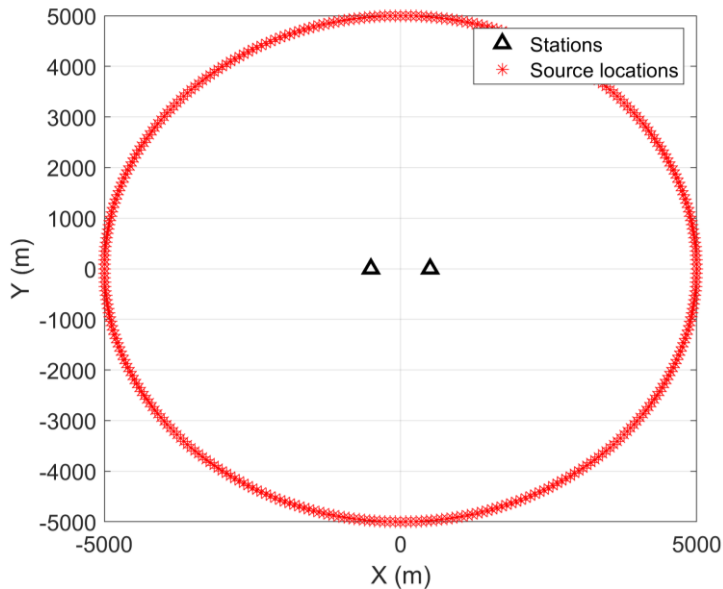
Related Literature: [Chmiel et al, 2019](#)



# Ambient noise interferometry

**Principle of ambient noise interferometry** : Ensemble average of seismic noise correlations over a sufficiently long measurement period approximates to the Green's function of the propagation medium (EGF)

- $EGF = -\frac{d}{2dt} (C_{AB}(t) + C_{AB}(-t))$  [Wapenaar 2004](#), [Weaver and Lobkis 2006](#)



- An isotropic illumination:
  - Actual distribution of sources at all azimuths
  - Diffuse wavefield
    - Inhomogeneity of the medium
    - Coda-wave interferometry

- A theoretical realization of noise seismograms measured for a propagation speed of 500 m/s at 3 Hz
- Station separation of 1000 m
- Sinusoidal behavior – Plane wave

- Phases cancel for  $180 - \theta_{FZ} > \phi > 0 + \theta_{FZ}$  and  $360 - \theta_{FZ} > \phi > 180 + \theta_{FZ}$
- $\theta_{FZ}$  is the Fresnel angle where constructive interference occurs

*Related Literature:* [Yao and van der Hilst 2009](#), [Yao, van der Hilst, de Hoop, 2006](#)

**Data preprocessing** : In order to diminish amplitude irregularities between stations and reduce impact of directional sources of noise in the data like earthquakes, we perform data preprocessing using temporal normalization and spectral whitening

- A running average temporal normalization is performed following

$$x_{norm}(t) = \frac{x(t)}{\sum_{m=t-\delta t}^t x(m)}; \text{ we chose } \delta t = 10 \text{ s}$$

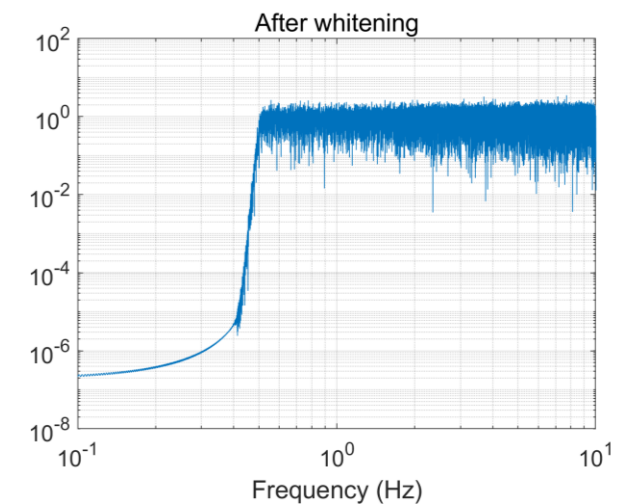
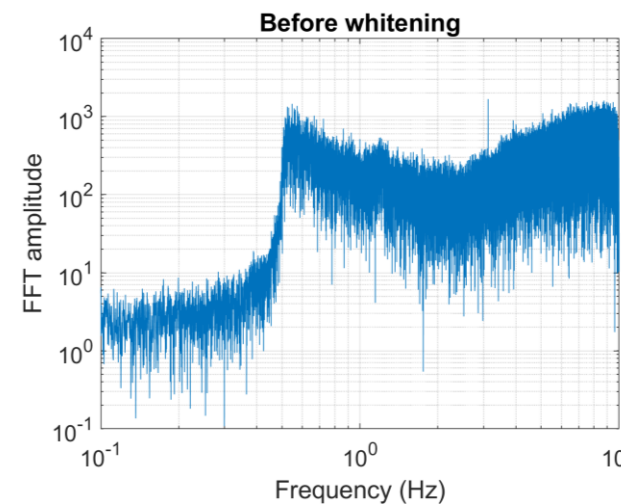
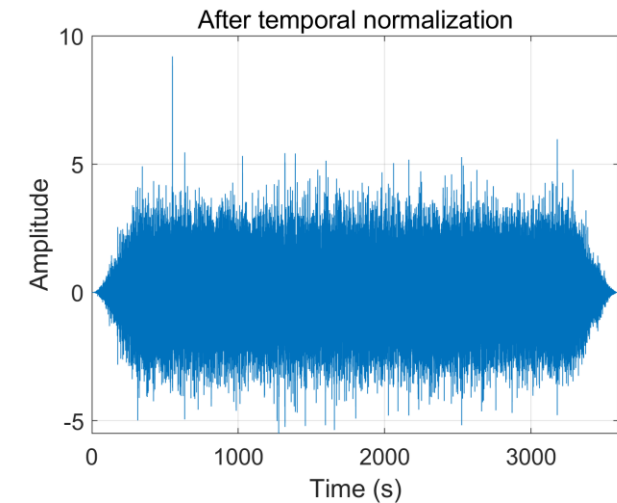
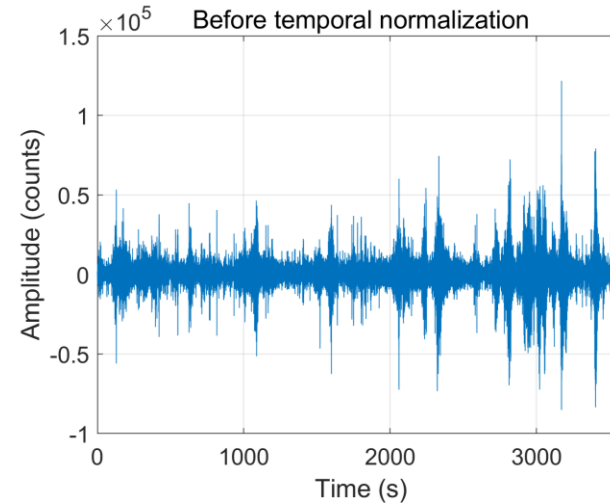
- Spectral normalization is performed by dividing the spectra with smoothed version of it,

$$X_{white}(f) = \frac{X(f)}{\sum_{m=f-\delta f}^{f+\delta f} X(m)}; \text{ we chose } \delta f =$$

0.001 Hz

- Additionally, a Tukey window with  $\alpha = 0.1$  is used prior to cross-correlating

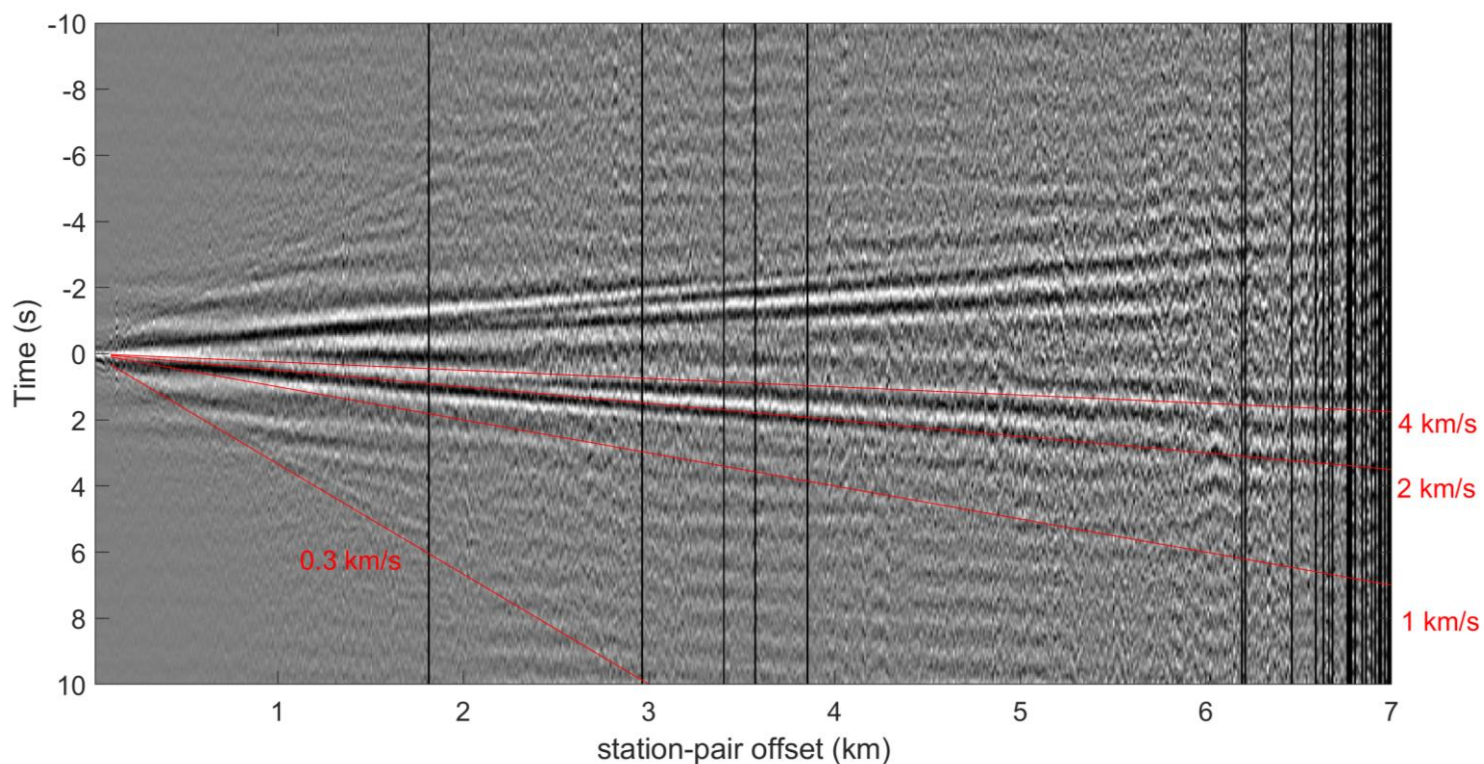
- We process the data in one-hour segments
  - Larger data-segments are useful for reducing effect of directional noise
  - On the contrary more ensemble averages are desired for convergence to Empirical Green's function
  - We found one-hour segments to perform well ([Seats et al 2012](#))



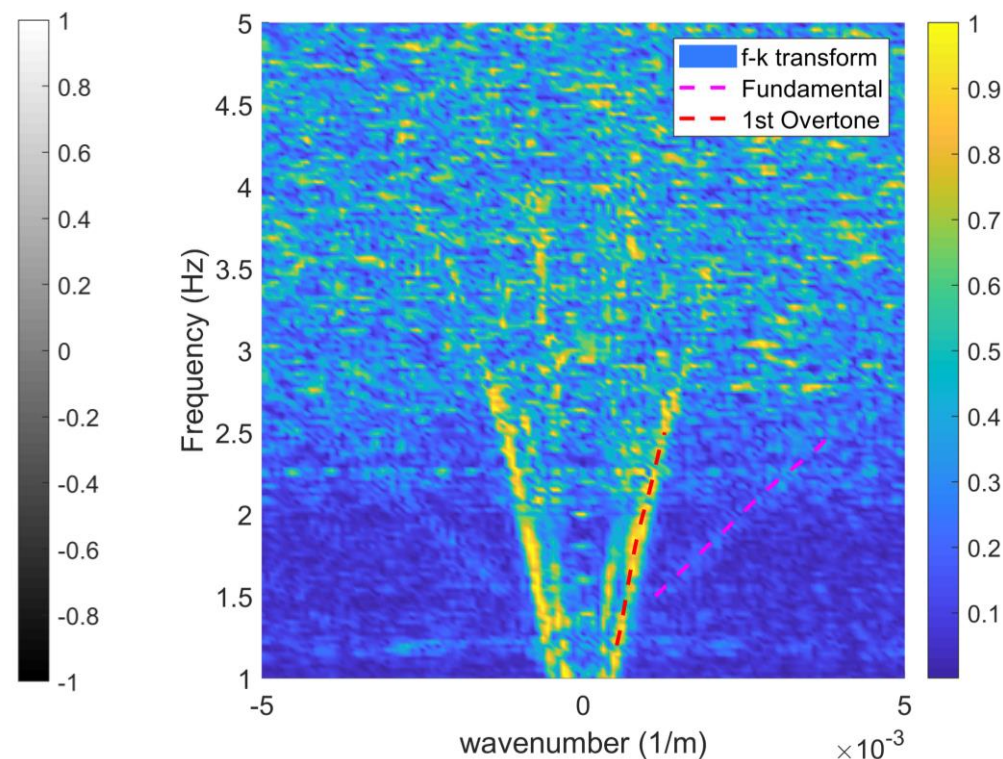


# Virtual noise gather

- Time-domain cross-correlations between station pairs are assembled in 25 m inter-station distance bins
- Although an azimuthal averaging occurs, but such a representation is important to appreciate the multimodal nature of surface waves at the site



- A symmetric nature of the CCF emerges – courtesy the azimuthal averaging
- Fast propagating higher order surface-wave modes at group speeds of 1-3 km/s (propagate deeper and prominently delineated at larger offsets)
- A weak fundamental mode is recovered (300-400 m/s) for shorter offsets



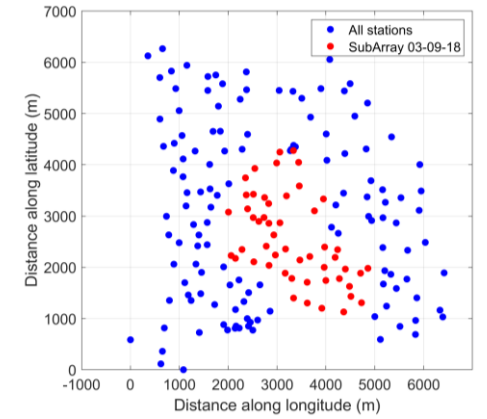
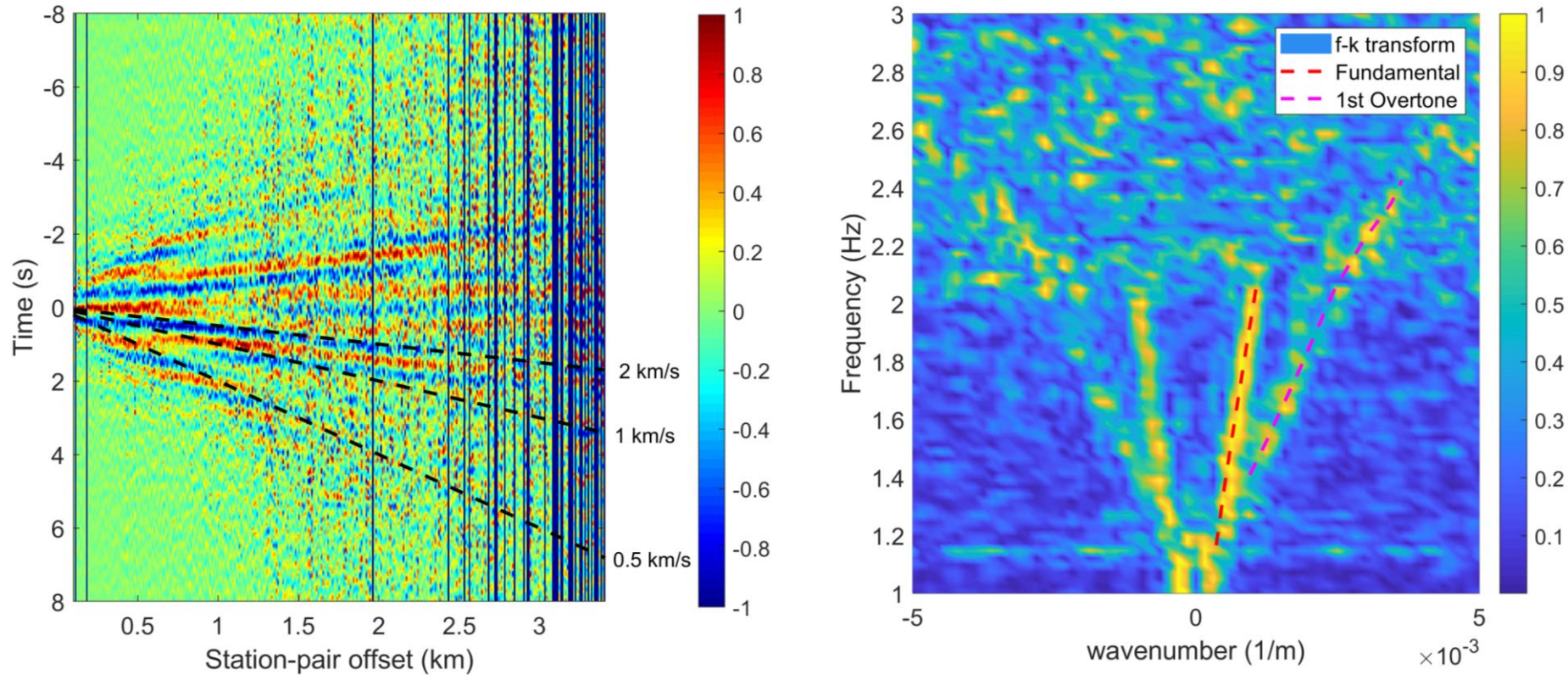
- The two different modes can be identified in the frequency-wavenumber domain
- Also establishes the fact that above 2.5 Hz, coherence diminishes drastically

Related Literature: [Mordret et al 2013](#),<sup>12</sup>  
[Chmiel et al 2019](#), [Roux et al 2016](#)




# Appreciating the multimodal nature – using subarrays

- A subarray processing is employed as a check to verify the presence of multiple modes

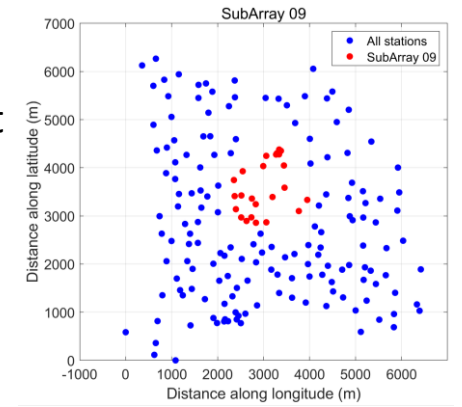
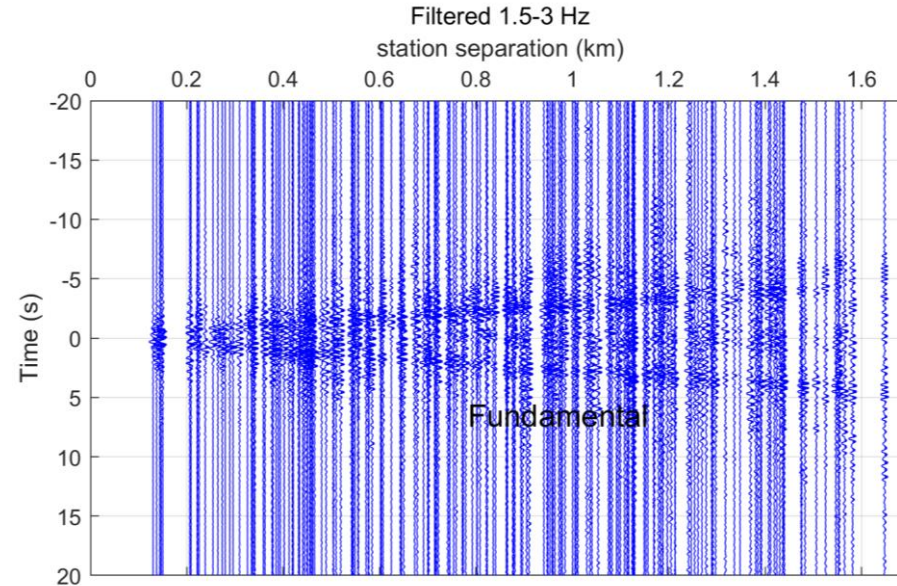
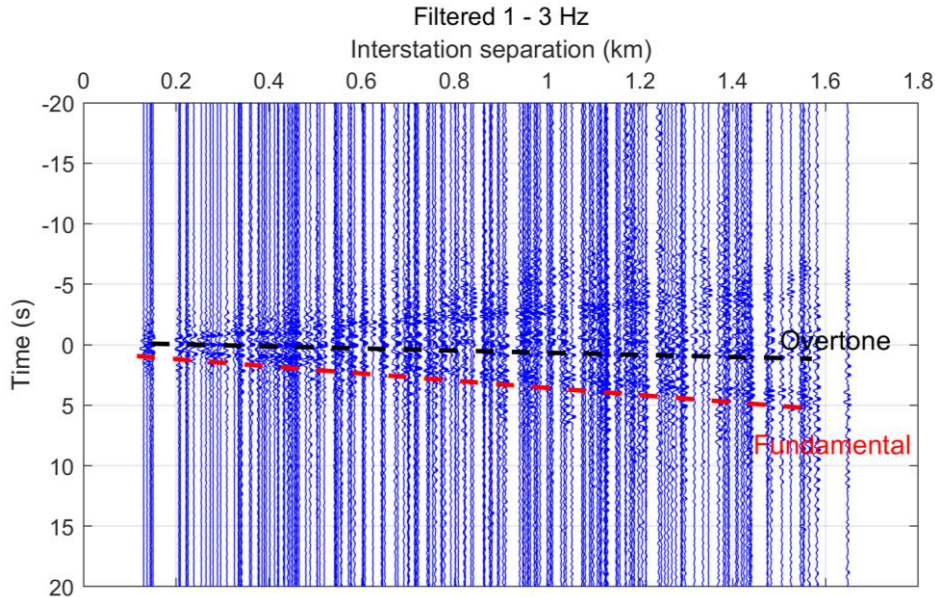


- A subgroup of stations for which both the modes are observed

- Majority of station-pairs with interstation-offset greater than a kilometer is dominated by the first overtone of surface waves
- Also, the first overtone is dominated for frequencies between 1-2 Hz; while the fundamental is marginally stronger for frequencies greater than 2 Hz  **More in next slide**

# Multimodal nature and frequency bands of interest

- For example, in subarray 09, cross-correlation gathers in frequency band 1.0-1.5 Hz is dominated by the first overtone and for frequencies between 1.5-2.5 Hz the fundamental mode dominates

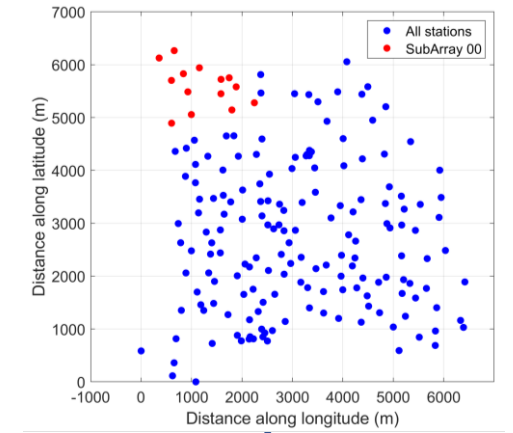
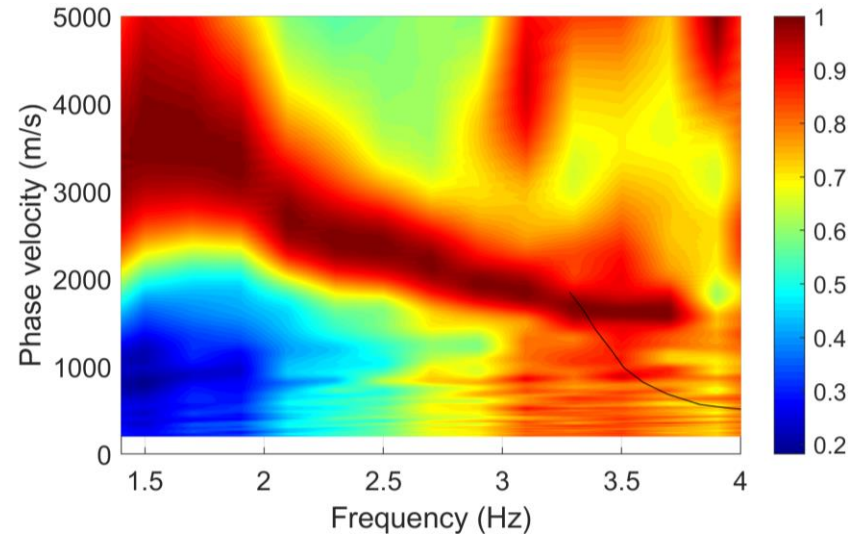
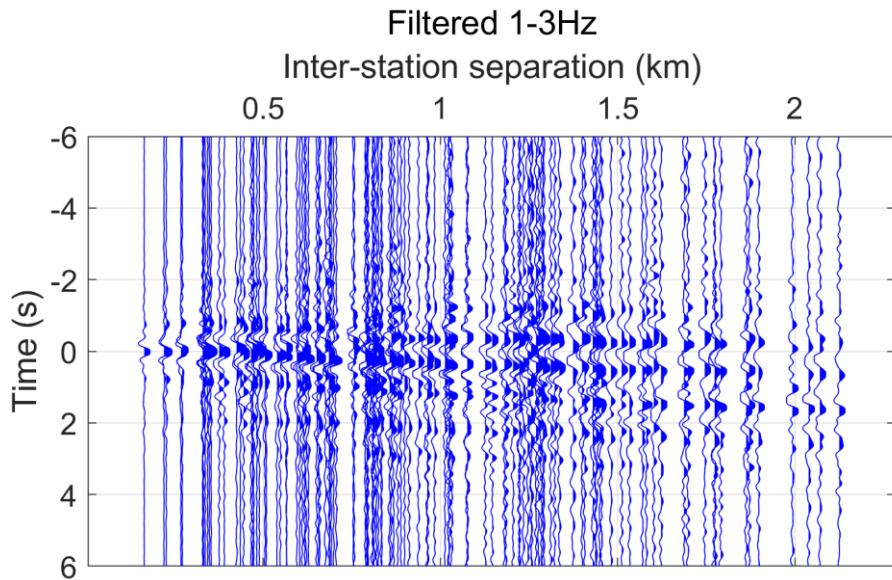


- An intuitive next step is to perform cross-correlation beamforming and obtain phase velocity distribution in different sub-arrays




# Cross-correlation beamforming

- We divide the area into several overlapping sub-arrays and obtain an initial estimate of sub-array phase velocities
- $P(f, p, \phi) = \sum_{i=1}^N X_i(f) e^{2\pi j f d_i \mathbf{k}}$ , where  $X_i(f)$  is the Fourier transform of the cross-correlation corresponding to the  $i^{th}$  station pair,  $d_i$  is distance between the station-pair and  $\mathbf{k} = [p \cos \phi \quad p \sin \phi]$  is the wave-vector



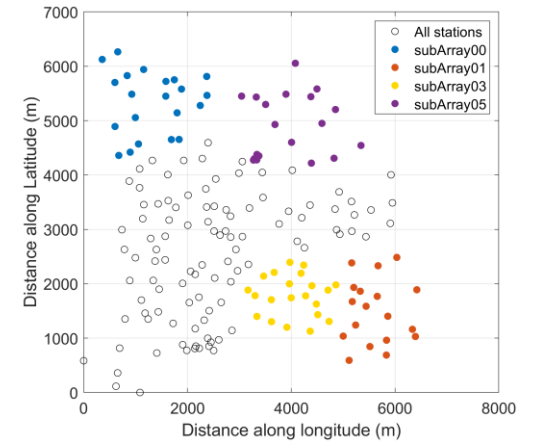
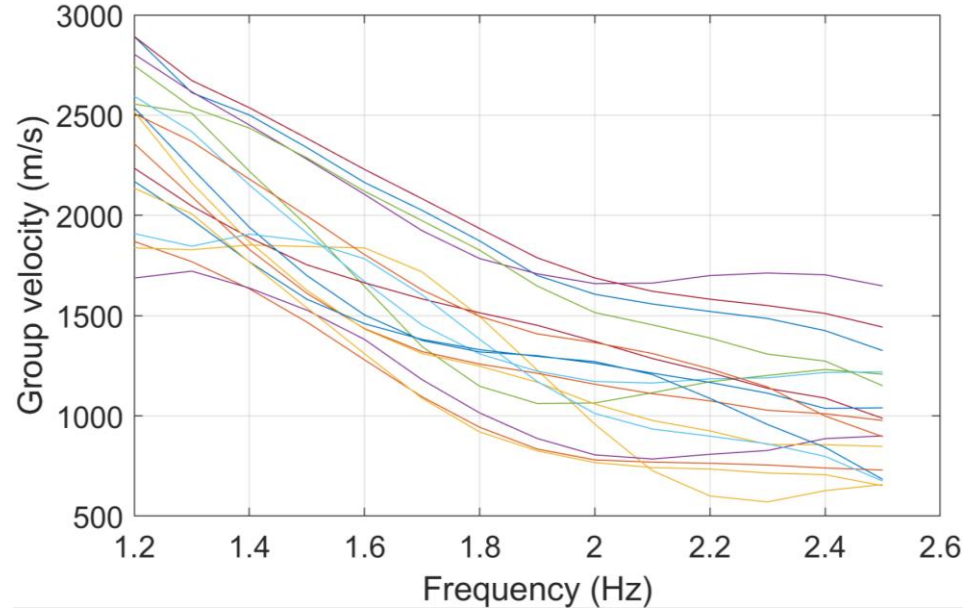
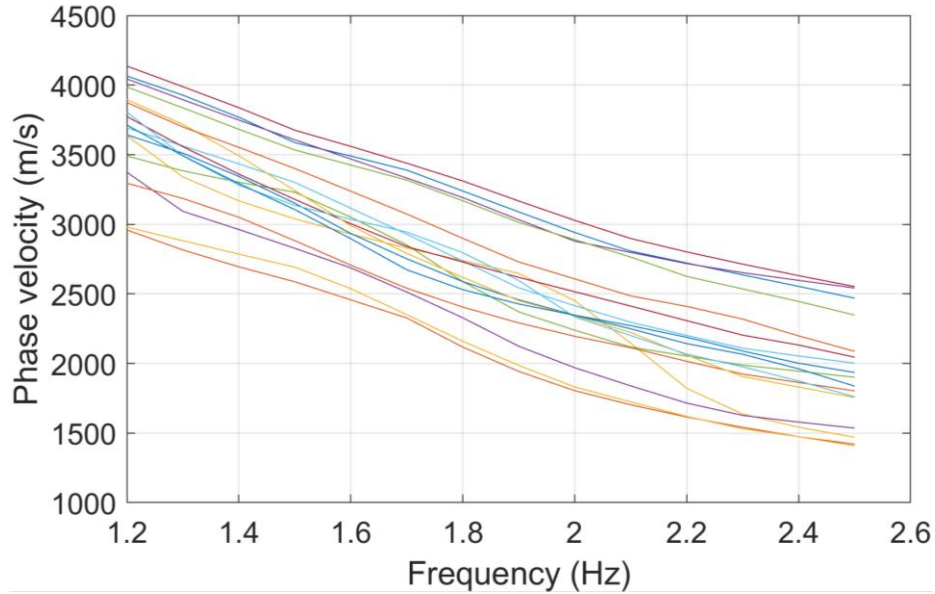
- A subgroup of stations for which the first overtone dominates

- It is important to observe the causal contribution of the CCF due to directional bias in the noise source distribution

- Phase velocities range between 2-4 km/s and a dispersive nature is observed
- This process is repeated for 18 of such overlapping subarrays  **more in next slide**

# Cross-correlation beamforming – subarray phase and group velocities

- Each subarray extends about 2x2 sq km and overlaps with surrounding arrays



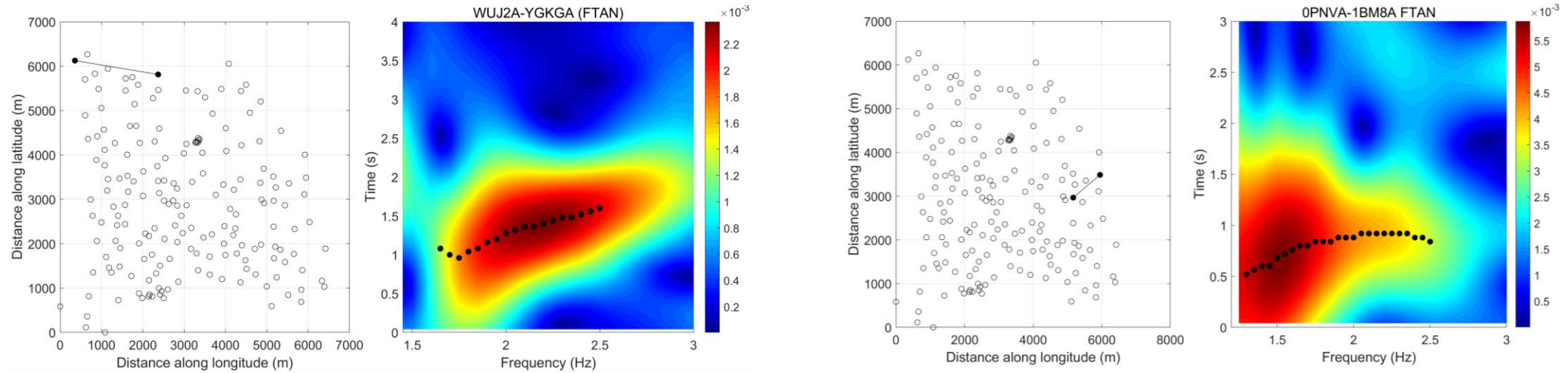
- Different subarray locations

- Phase velocities show significant changes in velocity between subarray
- Significant lateral inhomogeneity in the medium
  - Something to consider while doing tomography
  - An easy way to obtain a 3D model is to invert each of this dispersion curves and interpolate
    - Philosophical differences among peers (DBF, [Boue et al, 2013](#))

- Group velocity shows larger changes in velocity, since it is related to the gradient of phase velocity
- $$v_{grp} = \frac{v_{phase}}{\left(1 - \frac{\omega}{v_{phase}} \frac{dv_{phase}}{d\omega}\right)}$$
,  $\omega$  is angular frequency

# Towards tomography – Frequency-time analysis (FTAN)

- FTAN theory – Group velocities estimated at frequency  $\omega_0$  by using travel time corresponding to the peak of the envelope obtained as  $X(\omega_0, t) = IFFT(S_\omega(1 + \text{sgn}(\omega))G(\omega - \omega_0))$ , where  $S_\omega$  is the analytic CCF and  $G(\omega - \omega_0) = e^{-\alpha\left(\frac{\omega-\omega_0}{\omega_0}\right)^2}$  is a narrow-band gaussian filter.
- We chose  $\alpha$  to linearly vary between 30 and 50 starting at 1.2 Hz and ending at 2.5 Hz at intervals of 0.1 Hz. Essentially, the filter widens as frequency increases



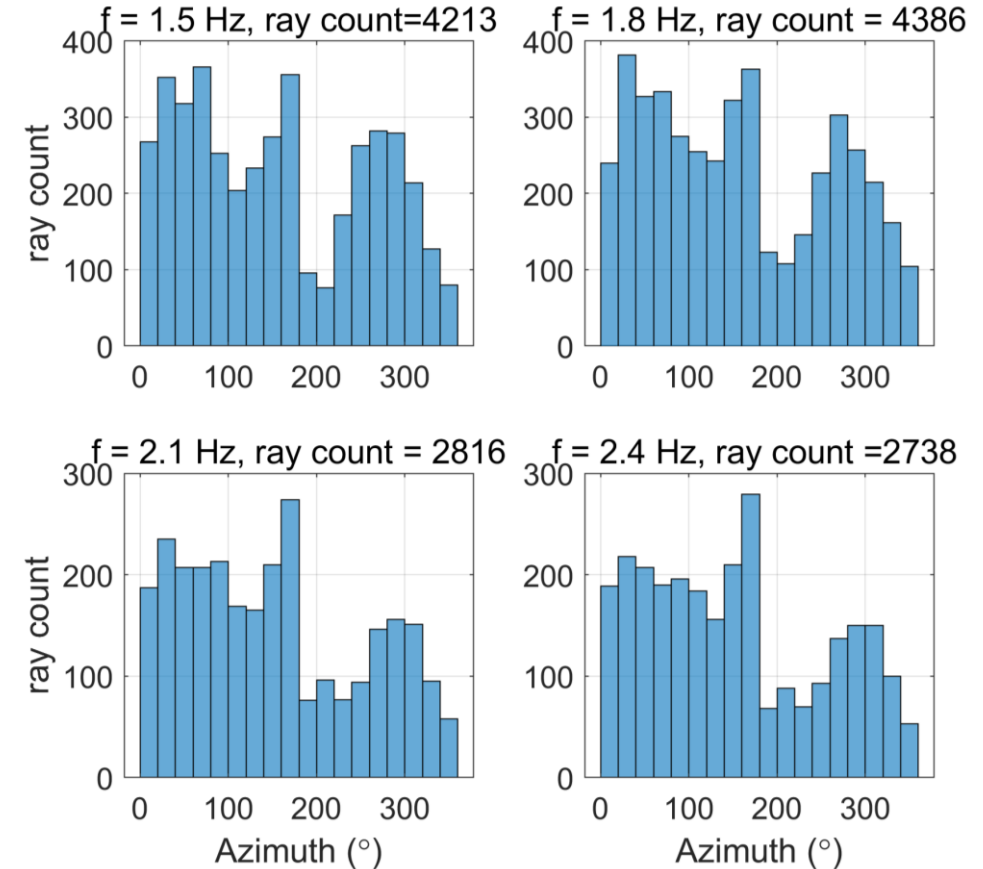
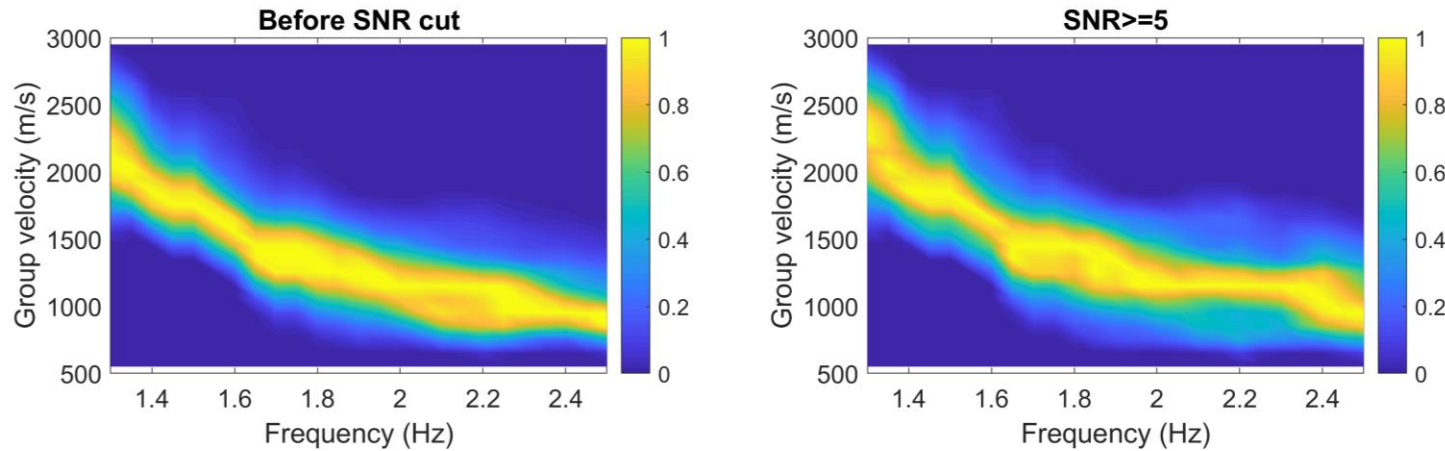
- FTAN above corresponds to the symmetric component of the CCF pertaining to different station-pairs, the locations of which are shown in the figures
- In principle, the FTAN travel times are derived separately for the causal and anti-causal part and only those frequency bins with deviations less than 20% travel time are considered
- The causal and anti-causal travel time differences are also used to construct the time-travel covariance matrix used during tomography

Related Literature: [Dziewonski et al, 1969](#),  
[Levshin & Ritzwoller, 2001](#)



# Towards tomography – Station pair selection

- Based on anti-causal and causal travel time difference of 20% and a spectral SNR of greater than 5 we select station pairs suitable for tomography
- Starting at 16,653 cross-correlation pairs
- We end up with about 4500 station pairs at 1.5 Hz and 2500 pairs at 2.5 Hz

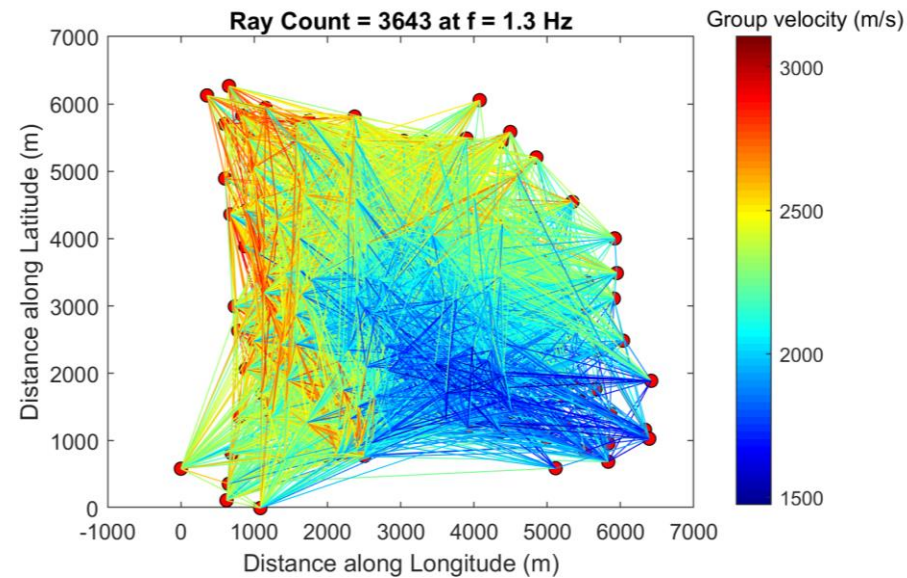
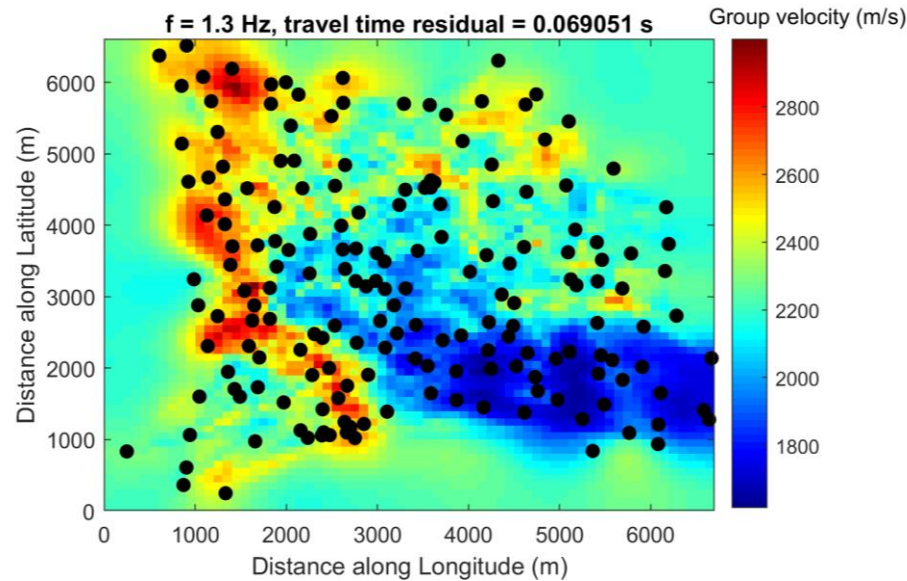


- A sufficient azimuthal distribution of station-pairs is achieved in the frequency band 1.3 – 2.5 Hz, which is necessary for tomography
- Criss-crossing rays per-cell are necessary for tomography in order to avoid directional bias in velocity estimates



# Straight ray tomography

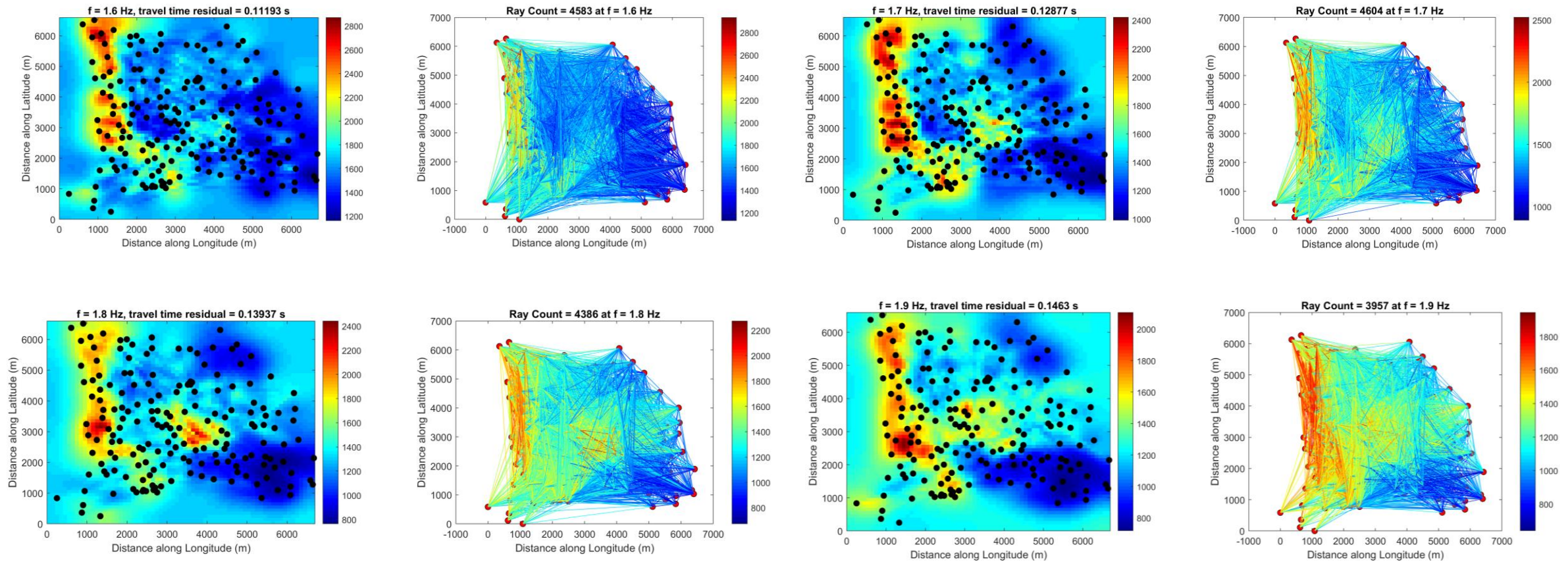
- Given the travel time  $t$  between a station pair at a frequency  $f$ , the theoretical travel time can be modeled as  $t = Gm$ , where  $G$  is a sparse matrix comprising the distance traveled by a ray in a cell. It is sparse, because only a few cells are traversed by a ray
- This problem is reformulated as  $\Delta t = G\Delta m$ , where  $\Delta m$  is a perturbation in model around the mean slowness  $m_0$
- Solution to this problem can be obtained by minimizing the penalty function
- $(Gm_0 - t)^T C^{-1} (Gm_0 - t) + \sum_k^N \alpha_k^2 |F_k(m_0)|^2 + \sum_k^N \beta_k^2 |H_k(m_0)|^2$
- $\Delta m = (\Delta t - Gm_0)^T C^{-1} (\Delta t - Gm_0) + m_0^T Q m_0$ , where  $Q = F^T F + H^T H$
- A detailed expansion of matrices  $F$  and  $H$  can be found in [Barmin et al 2001](#)
- We use smoothing parameters  $\alpha = 4000$ ,  $\beta = 300$ , and  $\sigma = 200$  [Goutorbe et al 2015](#) (open to debate, but should not change results considerably)
- Grid size =  $200 \times 200$  sq. m, Approximate ray-count per cell  $\approx 100$





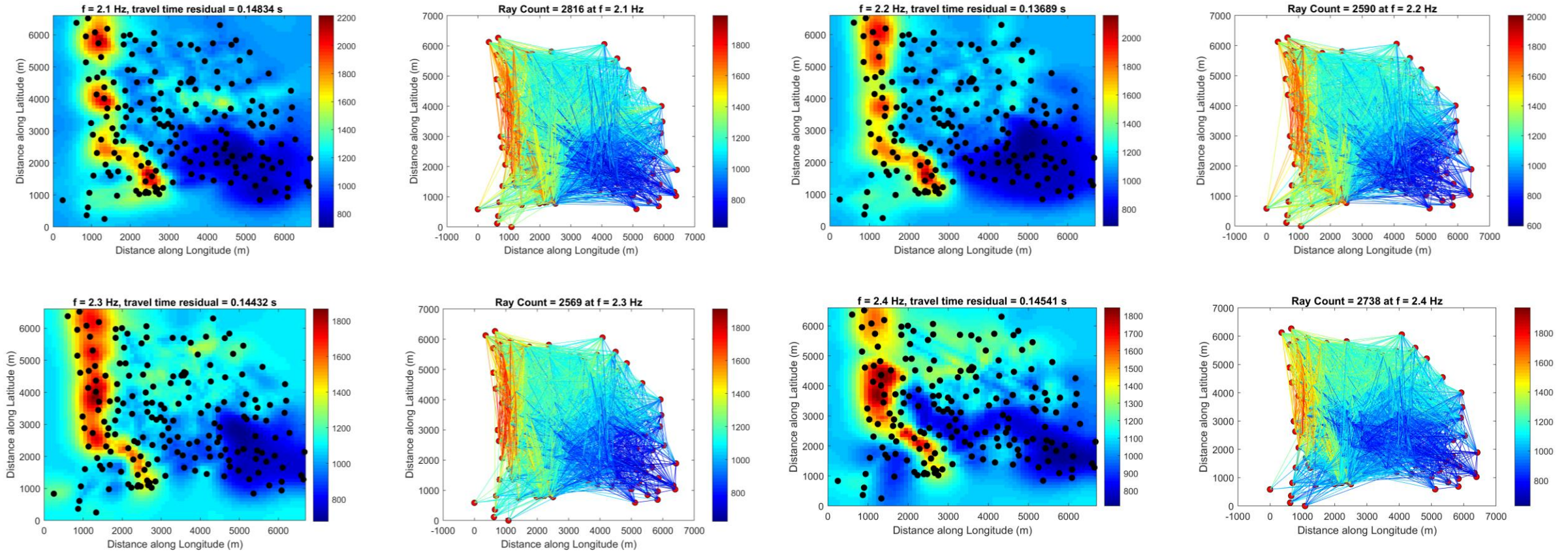
# Straight ray tomography (1.6-1.9 Hz)

- *A high velocity anomaly observed at western part of the array*
- *Low velocities observed in south-eastern part of the array*
- *Velocity perturbations of about 30% around the mean value – slightly high considering the philosophy behind the approach*
- *Spatial resolution of about 400 m is achieved*



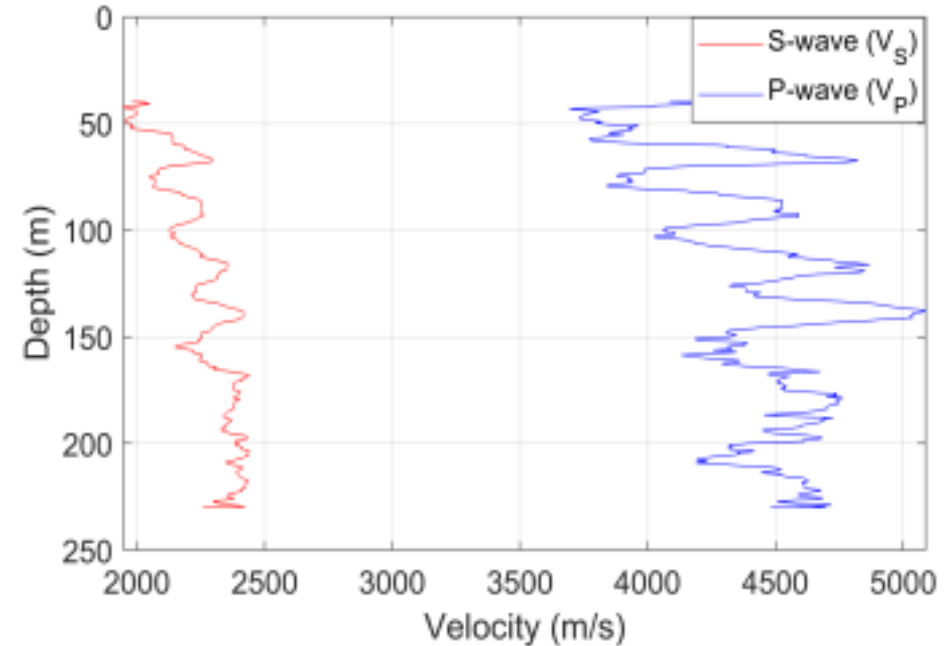
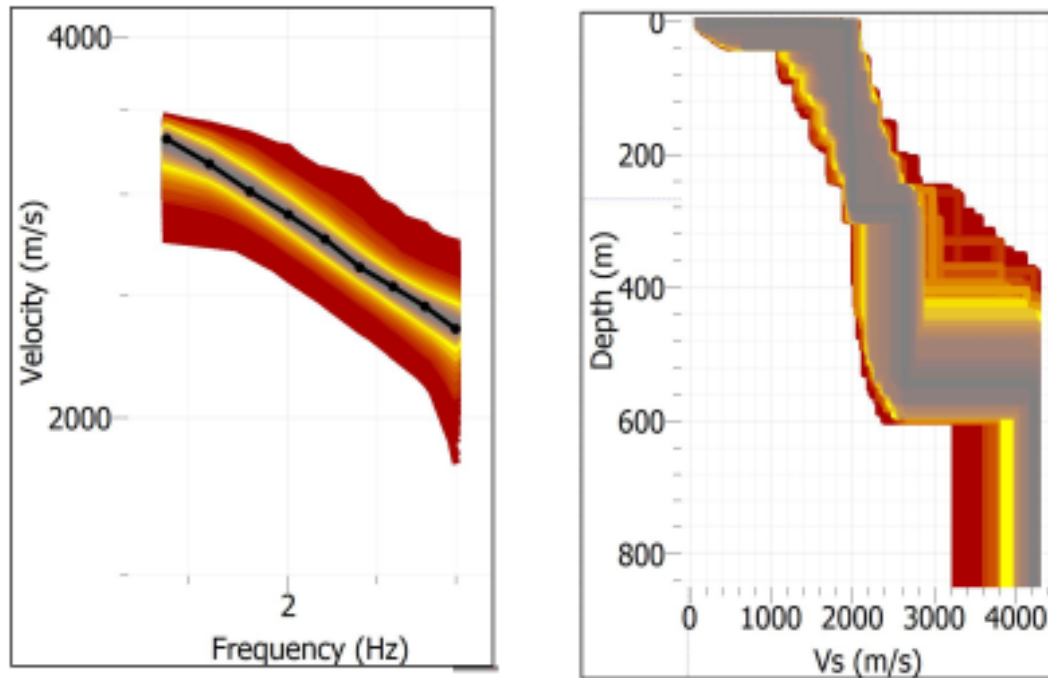
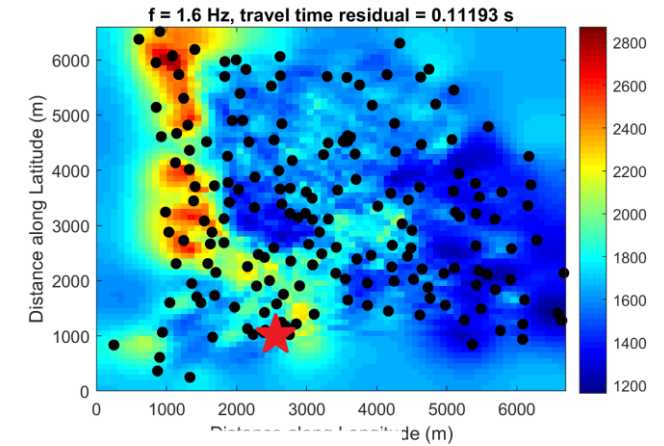


# Straight ray tomography (2.1-2.5 Hz)



# Preliminary inversion to depth at Cottessen

- A 1D depth inversion of the observed dispersion at Cottessen is performed
- Since the frequency band of dispersion is limited to about 2.5 Hz, we don't achieve a good shallow resolution
- For depth between 100-250 m, velocities from inversion are in agreement with those observed from logging



*Measured S-wave and P-wave velocity at Cottessen smoothed every 5 m (RWTH Aachen)*

*Figure: observed and fitted dispersion curve (left), explored S-wave velocity models (Geopsy)*

*Related Literature: [Wathelet et al 2004](#), [Sambridge, 1999 \(I\)](#), [Koley et al 2022](#)*

# Research questions to be addressed

- *Shallow subsurface geology information necessary to facilitate transformation from frequency to depth*
  - *Especially P-wave velocity and density (RWTH Aachen)*
- *Realization of an optimal array configuration that would ensure analysis of a wider frequency band of interest and ability to perform tomography*
  - *Handling of overtones, body waves, anisotropic illumination etc – Work ongoing*
  - *Necessity to be able to analyze frequencies as high as 5 Hz, need for denser sampling*
- *Development of an MCMC (Metropolis-Hastings) code to perform the inversion – done!*
- *Check on the usage of Eikonal tomography, phase-front tracking*
- ***Acquisition improvements***
  - ***Ensure stations have better data – current installations had poor low-frequency sensitivity***
  - ***Ensure better coupling of sensors to the ground***
  - ***Field tests with software running is necessary before actual deployment***





# Questions

---

